# Dynamical real-space renormalization group calculations with a highly connected clustering scheme on disordered networks

D. Balcan[1] and A. Erzan[1,2]
[1]*Department of Physics, Faculty of Sciences and Letters, Istanbul Technical University, Maslak 34469, Istanbul, Turkey*
[2]*Gürsey Institute, P.O. Box 6, Çengelköy, 34680 Istanbul, Turkey*
(Received 31 August 2004; revised manuscript received 10 December 2004; published 28 February 2005)

We have defined a type of clustering scheme preserving the connectivity of the nodes in a network, ignored by the conventional Migdal-Kadanoff bond moving process. In high dimensions, our clustering scheme performs better for correlation length and dynamical critical exponents than the conventional Migdal-Kadanoff bond moving scheme. In two and three dimensions we find the dynamical critical exponents for the kinetic Ising model to be $z=2.13$ and $z=2.09$, respectively, at the pure Ising fixed point. These values are in very good agreement with recent Monte Carlo results. We investigate the phase diagram and the critical behavior of randomly bond diluted lattices in $d=2$ and 3 in the light of this transformation. We also provide exact correlation exponent and dynamical critical exponent values on hierarchical lattices with power-law and Poissonian degree distributions.

DOI: 10.1103/PhysRevE.71.026130 PACS number(s): 05.50.+q, 64.60.−i

## I. INTRODUCTION

We have generalized the dynamical real-space renormalization group (RSRG) calculations for the kinetic Ising model [1] to dilute lattices with arbitrary number of nearest neighbors, motivated by an interest in the relaxation behavior of networks [2] with power-law and Poisson degree distributions. We propose a different clustering scheme which improves, but does not completely fix, the problematic behavior at high dimensions of the RSRG. This scheme yields very accurate dynamical exponents in two and three dimensions.

We first computed the dynamical critical exponent $z$ in the Migdal-Kadanoff bond moving scheme [3,4] on networks with arbitrarily high, but uniform, connectivity and found, as have others [5,6], that $z$ gradually converges to unity, as the spatial dimension of the system becomes very large (for $d=12$, $z-1=10^{-5}$) and the correlation length exponent converges to $\nu=1$ (see Figs. 1 and 2). This is in contrast to the expected mean-field values of $\nu=0.5$ and $z=2$ above the upper critical dimension. The dynamic RSRG calculation thus yields neither a sharp crossover above the upper critical dimension, $d_c=4$, nor the correct mean-field (MF) behavior in the high-dimension limit. We have observed that a static RSRG calculation with Migdal-Kadanoff (MK) bond moving scheme also converges to the same limits, but it does so from above, whereas the dynamical RSRG calculation does so from below (see Fig. 2).

The pathalogical behavior of RSRG in high dimensions, at low temperatures, has been remarked upon by several authors [7,8]. To our knowledge, no RSRG scheme of bond-moving, cluster, or majority rule type is able to display the sharp crossover to MF critical exponents at the upper critical dimension of the system under consideration (except for the so-called "hierarchical" Hamiltonians [9]). It should be remembered that the upper critical dimension has been identified in the context of the momentum-space renormalization group in the manner of Wilson and Kogut [10], where it can be obtained from simple power counting in momentum-space integrals for the appropriate renormalized vertices (interactions) to decide whether they are relevant or irrelevant [11].

The reason why the MK approach fails to provide a reasonable approximation to the critical behavior of $d$-dimensional hypercubic lattices in large $d$ is twofold. The first is because it increasingly underestimates the contribution from the loops in the $d$-dimensional Euclidean lattice and this effect leads to more and more inaccurate results for large dimensions. The second, and again topological, reason for the divergence of MK results from those on Euclidean hypercubic lattices is the nonuniform connectivity of the underlying "hierarchical lattice," on which the MK scheme for RSRG is realized as an exact transformation [12,13] (see Fig. 3). We turn this feature to an advantage in investigating the dynamical behavior of the Ising model on networks with power-law degree distributions.

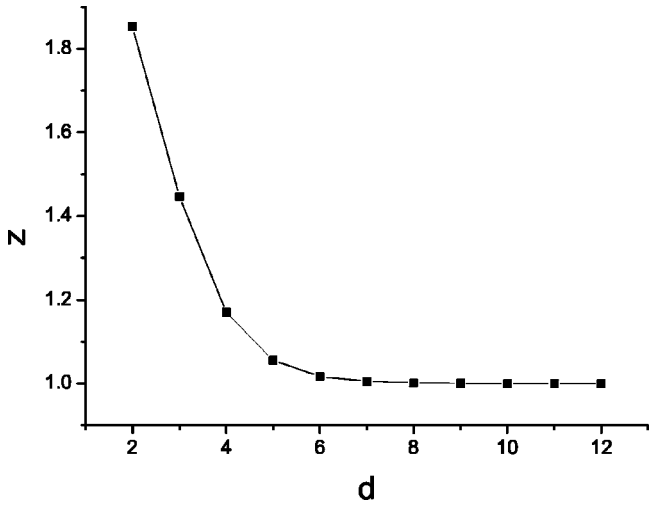


FIG. 1. The dynamical critical exponent $z$ versus dimension $d$ obtained via the conventional Migdal-Kadanoff bond moving scheme, with scale factor $\lambda=2$. For large $d$, $z$ converges to 1.

 

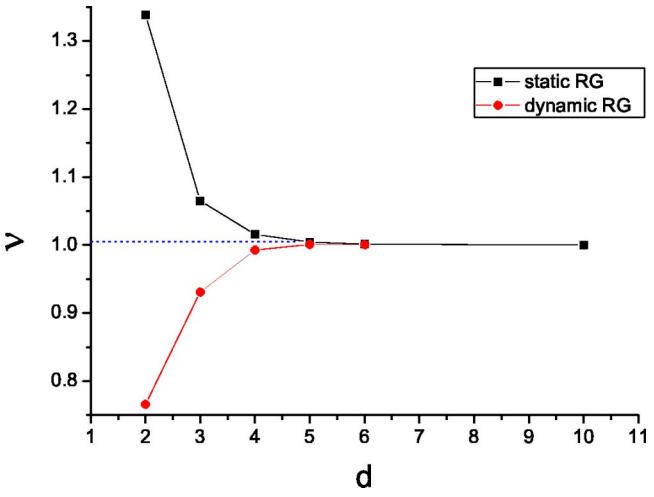


FIG. 2. The correlation critical exponent $\nu$ versus dimension $d$ via the conventional Migdal-Kadanoff bond moving scheme, with scale factor 2. It can be seen that $\nu$ converges to 1 for large $d$.

It is no surprise that the conventional MK bond moving scheme should not yield faithful results at high dimensions, since the whole strategy here [4] is to deform the lattice in such a way that the neighborhood of the spins to be decimated locally looks like a *one-dimensional* chain and the partial sums can be done exactly. Although the total number of bonds connecting spin pairs is conserved under this operation, the number of loops is not, and the topology of the resulting network is completely different [Figs. 3(a)–3(c)] We have found a way to improve the performance of the RSRG approach in relation to $d$-dimensional hypercubic lattices by defining a type of cluster which retains the interconnectivity of the moved spins [Fig. 3(d)]. These improvements do not remove, of course, the Griffiths singularities and problems with non-Gibbsian measures, etc. [7,13]. These come from the diverging connectivity at an infinite number of vertices of the hierachical lattice, obtained by replacing each bond iteratively with the clusters seen spanning the edges of the bond-moved unit cell in Figs. 3(c) and 3(d).

We were able to obtain a convergence, with two digit accuracy, to $\nu=0.63$ for high dimensionality ($d>13$), a result which is at least smaller than 1 but still larger than the correct MF result ($\nu^{\mathrm{MF}}=0.5$) (see Fig. 4). Likewise, the dynamical critical exponent in this scheme converges to the value 1.6 for dimensions $d\geqslant 11$ (Fig. 5). These results are summarized in Table I. The clustering scheme for the RSRG also performs very well in low dimensions (Table II). The dynamical exponent calculated within our scheme for $d=2$ is $z=2.13$ and for $d=3$ is $z=2.09$, to be compared with the best simulation results [14–20], which give values between 2.11 and 2.24 for $d=2$ and between 2.01 and 2.11 for $d=3$ (Table III).

Going over to the dynamical critical behavior for bond-diluted lattices, we first applied the dynamic RSRG technique to the bond-diluted kinetic Ising system in two and three dimensions. The approximation we used to compute the configuration averages is in fact exact for annealed randomness. The approximate transformations for the dilution parameter $p$ and the coupling constant are well behaved as

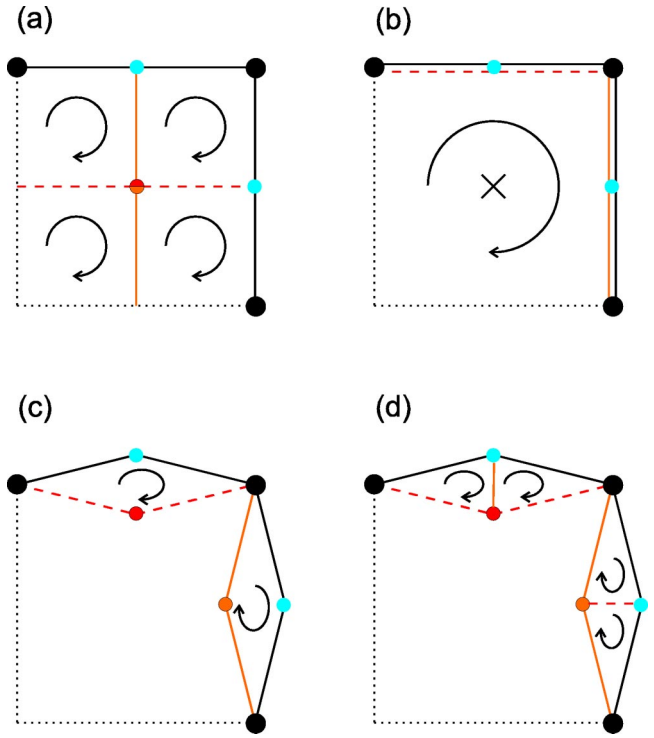


FIG. 3. (Color online) A comparison of the conventional MK bond moving and our clustering scheme, for $d=2$ and $\lambda=2$. (a) A square lattice, with nested unit cells of linear sizes 1 and 2. The "corner spins," which will survive the decimation procedure, are shown in black. The spin at the center is connected to four different neighbors, and there are four loops (or plaquettes). (b) The result of bond moving. The red (dashed) bonds have been moved vertically, the orange (light grey) bonds horizontally. The spin at the center is disconnected (it just contributes a trivial $k_BT\ln 2$ term to the free energy), and there is now just one loop. (c) The central spin has been "split" into two and moved together with the red and orange bonds, so that the number of distinct interacting spin pairs is conserved. This method yields a renormalization group transformation which is equivalent, to leading order, to that in case (b). (d) Beyond just "splitting" the spin at the center of the square and moving it together with the red and orange bonds, the connectivity between this central spin and its neighbors has been preserved. In this case, the number of distinct pairs of interacting spins is not conserved, but the number of loops is. The "hierarchical lattices" on which the renormalization group transformations considered here are exact, are obtained by iteratively replacing each bond in (c) or (d) with the whole cluster connecting the two corner spins. Shown here is only the case without any bond dilution.

one approaches the separatrix, or critical line, from above, but the approximation breaks down in the ordered phase and for low temperatures in the disordered phase. In both two and three dimensions we were able to compute the RG flows on the disordered side of the separatrix and on the separatrix itself, and thereby determine the phase diagrams. In two dimensions we find a disorder fixed point, which is unstable and which we interpret as a tricritical point, since there the second-order phase transition line gives way to a first-order transition line. The pure Ising fixed point is stable and determines the exponents along the second-order transition line. In three dimensions, no disordered critical fixed point is

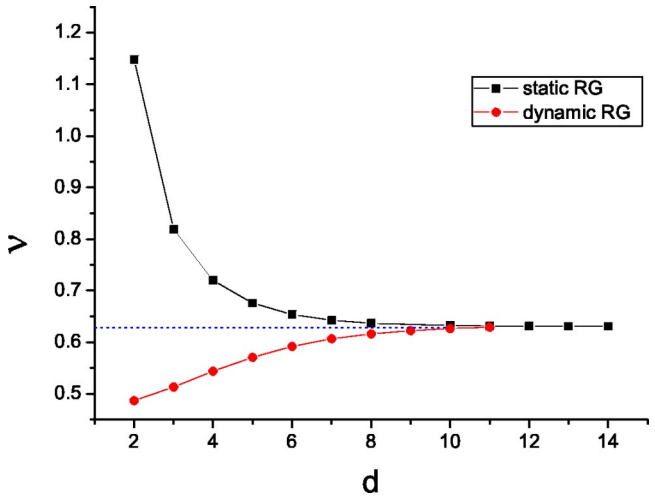


FIG. 4. The correlation critical exponent $\nu$ versus dimension $d$ obtained by our clustering scheme. $\nu$ converges to 0.63 for large $d$ (to be compared with Fig. 2). See Table I.

found. The critical line is depressed to zero temperature at a concentration $p_e > p^*$, where $p^*$ is the percolation fixed point. The flow along the critical line is to the pure Ising fixed point at $p=1$, and thus the critical exponents along the critical line are the same as the pure Ising exponents, also in three dimensions. Computing the effective critical exponents along the critical line, we find that $z_{\text{eff}}$ varies nonmonotonically as a function of $p$, within the intervals [2.01,2.25] for $d=2$ and [2.09,2.69] for $d=3$ (see Fig. 6).

Our scheme as well as the conventional equilibrium Migdal-Kadanoff RSRG (see also Refs. [21,22]) fails to predict the crossover to a disorder critical fixed point for $d=3$, both demonstrated by means of finite-size scaling arguments [23] applied to large Monte Carlo simulations [24] and expected on the basis of the Harris criterion [25]. The value we find for the pure system specific heat exponent $\alpha$ via the hyperscaling relation $2-\alpha=d\nu$ in $d=3$ is negative for the

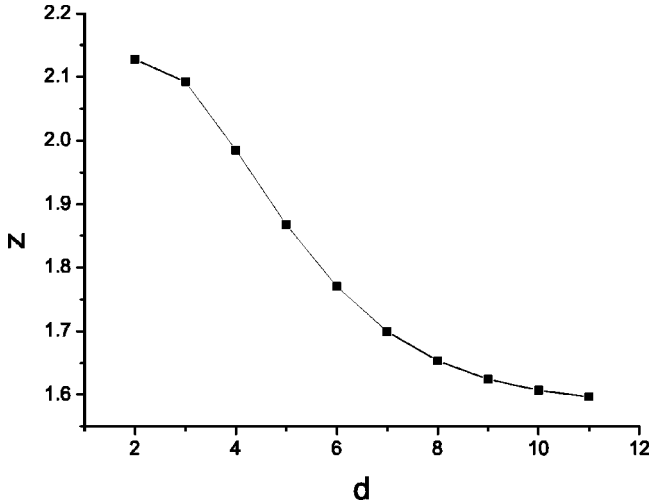


FIG. 5. The dynamical critical exponent $z$ versus dimension $d$ obtained by our clustering scheme. $z$ converges to 1.6 for large $d$ (to be compared with Fig. 1). See Table I.

TABLE I. Our results for dynamical critical exponent $z$ and correlation critical exponent $\nu$ with respect to space dimension $d$ at the pure Ising fixed point.

| $d$ | $z$ | $\nu_{\text{dynamic}}$ | $\nu_{\text{static}}$ |
|---|---|---|---|
| 2 | 2.13 | 0.49 | 1.15 |
| 3 | 2.09 | 0.51 | 0.82 |
| 4 | 1.99 | 0.54 | 0.72 |
| 5 | 1.88 | 0.57 | 0.68 |
| 6 | 1.77 | 0.59 | 0.65 |
| 7 | 1.70 | 0.61 | 0.64 |
| 8 | 1.65 | 0.62 | 0.64 |
| 11 | 1.60 | 0.63 | 0.63 |

static RSRG calculation for $\nu$, while the dynamic calculation yields a positive $\alpha$. These results have to be interpreted in the context of the still ongoing debate on the criteria for the stability of the pure-system critical behavior. The rather extensive literature on the Harris criterion [25] has been recently reviewed by Janke and Weigel [26]. It has been shown by various authors [22,27,28] that the Harris criterion, which equates the crossover exponent for randomness $\phi$, to the pure system $\alpha$, is simply not applicable on hierarchical lattices, and various alternative criteria, such as the "wandering exponent" [27] for correlations in the nonperiodic variations in the number of bonds incident on lattice points (the degree of the node), have been proposed. The calculation of this exponent for our present RSRG scheme goes beyond the scope of this paper and will be considered in a separate publication.

The paper is organized as follows. In the next section we set up the dynamical RSRG calculations for bond-diluted hypercubic lattices, and introduce a clustering scheme on which we will implement it. The last section includes our results and a discussion of the relevance of our results to nonuniform lattices with power-law and Poissonian degree distributions.

## II. DYNAMICAL RSRG CALCULATIONS FOR BOND-DILUTED HYPERCUBIC LATTICES

In order to investigate the effect of the underlying lattice of arbitrarily high degree on dynamical behavior of an interacting system residing on this lattice, we consider an Ising model on the nodes of a hypercubic lattice of $d$ dimensions,

TABLE II. The fixed points and the critical exponents in $d=2$ and $d=3$. The first value of $p$ shows the pure Ising fixed point; the second one shows the percolation fixed point for each dimension $d$.

| $d$ | $p$ | $K^*$ | $\nu_p$ | $\nu_{\text{dynamic}}$ | $\alpha_{\text{dynamic}}$ | $z$ |
|---|---|---|---|---|---|---|
| 2 | 1 | 0.27 | - | 0.49 | 1.03 | 2.13 |
| | 0.5 | 0.82 | 1.43 | 0.48 | 1.04 | 2.16 |
| 3 | 1 | 0.12 | - | 0.51 | 0.46 | 2.09 |
| | 0.16 | - | 1.01 | - | - | - |

TABLE III. Comparison of our results with the known values coming from different approaches. Here dynamical RSRG calculations are written as DRSRG and Monte Carlo studies are denoted by MC.

| $d$ | Reference | Method | $z$ |
|---|---|---|---|
| 2 | Present work | DRSRG | 2.13 |
| | Stauffer [14] | MC | 2.18 |
| | Nightingale and Blöte [15] | MC | 2.17 |
| | Li *et al.* [16] | MC | 2.13 |
| | Lauritsen and Ito [17] | MC | 2.13±0.02 |
| | Mülker *et al.* [18] | MC | 2.21±0.03 |
| | Droz and Malaspinas [6] | DRSRG | 1.85 |
| 3 | Present work | DRSRG | 2.09 |
| | Ito *et al.* [19] | MC | 2.06 |
| | Stauffer [14] | MC | 2.04 |
| | Lauritsen and Ito [17] | MC | 2.04±0.03 |
| | Mülker *et al.* [18] | MC | 2.08±0.03 |
| | Ito [20] | MC | 2.06±0.02 |
| | Droz *et al.* [6] | DRSRG | 1.45 |
| 6 | Present work | DRSRG | 1.77 |
| | Droz and Malaspinas [6] | DRSRG | 1.02 |

which will be subjected to bond dilution to yield a disordered network with a Poisson degree distribution.

The Hamiltonian of the system is given by

$$H = -\sum_{\langle ij \rangle} J_{ij}\sigma_i\sigma_j, \tag{1}$$

where $J_{ij}$ is the interaction between two nearest-neighbor spins and $\sigma_i$ is the spin variable which can take the values $+1$ and $-1$. The sum is taken over all nearest-neighbor pairs.

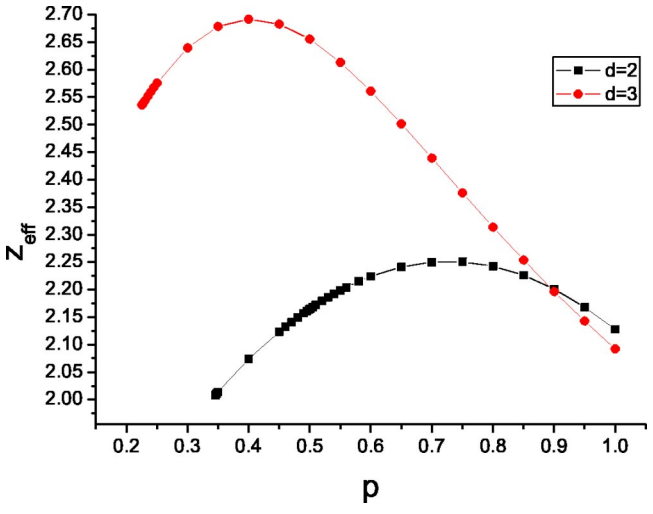


FIG. 6. The effective dynamical critical exponent $z_{\text{eff}}$ versus the bond occupation probability $p$, obtained by our clustering scheme. The intervals along the $p$ axis sampled by more points correspond to the intervals around the fixed point or to the end points of the validity of the RG transformation.

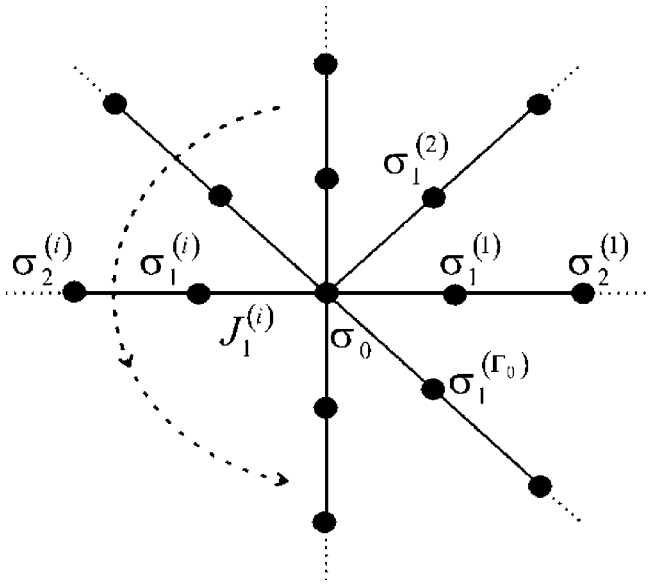


FIG. 7. We generalize the notation of Suzuki *et al.* [1] to the case of a $d=\Gamma_0/2$ dimensional hypercube. The"corner spin" on which we concentrate is denoted by $\sigma_0$, and on the original lattice (without bond moving) its $j$th-neighbor spin in the $i$th direction is denoted by $\sigma_j^{(i)}$, where $i=1,2,\ldots,\Gamma_0$ in the counterclockwise direction. Thus $\sigma_1^{(i)}$ and $\sigma_2^{(i)}$ are, respectively, the first and second nearest neighbors of $\sigma_0$, in the $i$th direction. The coupling constant $J_1^{(i)}$ is also shown.

In a $d$-dimensional hypercubic lattice, the number of nearest neighbors of a spin is $\Gamma_0=2d$ on the pure lattice.

In order to be able to derive the equation of motion for the magnetization of a given spin—say, $\sigma_0$—we would like to introduce some notation and relabel the spins in its neighborhood in a systematic way. This is shown in Fig. 7, where we denote the $j$th neighbor in the $i$th lattice direction as $\sigma_j^{(i)}$, with $i=1,\ldots,\Gamma_0$. The interaction constant between the spins $\sigma_0$ and $\sigma_1^{(i)}$ is denoted by $J_1^{(i)}$. All the coupling constants are independently and identically distributed—e.g.,

$$P(J_1^{(i)}) = p\,\delta(J_1^{(i)} - J) + (1-p)\,\delta(J_1^{(i)}). \tag{2}$$

### A. Equation of motion for the magnetization

Using Glauber dynamics [29] we may write down the equation of motion for the magnetization $m_0 \equiv \langle \sigma_0 \rangle$ and get

$$\frac{d}{dt}m_0(t) = -m_0(t) + \left\langle \tanh\left( \sum_{i=1}^{\Gamma_0} K_1^{(i)}\sigma_1^{(i)} \right) \right\rangle, \tag{3}$$

where $K_1^{(i)} \equiv \beta J_1^{(i)}$ and $\beta \equiv (k_B T)^{-1}$. Here the brackets $\langle \cdots \rangle$ denote both the thermal expectation value and the configuration average over the bond randomness.

The strategy is now to expand the function appearing inside the brackets in Eq. (3) in terms of spin products. The first term is linear in the spins. To be able to proceed further, we have to make the crucial approximation of taking the thermal averages over the spins $\sigma_1^{(i)}$ and the configurational averages over the bonds $K_1^{(i)}$ independently of each other.

This amounts to making a mean field or effective medium type of approximation, neglecting the fluctuations in the bond configurations neighboring different spins. Moreover, since the thermal averages are implicitly calculated with respect to some average interaction strength, this represents an annealed approximation to the original quenched problem. These simplifications were also made by Droz and Malaspinas [6,21]. The assumption is that the difference between the annealed and quenched averages and the departures from the effective medium approximation will be higher-order effects, and not contribute to the scaling behavior of the equation of motion to leading order.

Since the number $\Gamma$ of connected nearest neighbors of any lattice point on this disordered lattice will be distributed according to

$$P(\Gamma) = \sum_{n=0}^{\Gamma_0} \binom{\Gamma_0}{n} (1-p)^n p^{\Gamma_0 - n} \delta(\Gamma - (\Gamma_0 - n)), \tag{4}$$

we get

$$\left(1 + \frac{d}{dt}\right) m_0(t) = \left[ \sum_{\Gamma=1}^{\Gamma_0} \binom{\Gamma_0 - 1}{\Gamma - 1} p^{\Gamma} (1-p)^{\Gamma_0 - \Gamma} a_{\Gamma}(K) \right] \times \sum_{i=1}^{\Gamma_0} m_1^{(i)} + g(p,K,t), \tag{5}$$

with $m_1^{(i)} \equiv \langle \sigma_1^{(i)} \rangle$ and $K \equiv \beta J$. Here $a_\Gamma(K)$ is the coefficient of the first-order term coming from the expansion of the hyperbolic tangent in terms of products of spin variables, for a particular realization of the disorder in which the spin $\sigma_0$ has $\Gamma$ nearest neighbors. These coefficients are given by

$$a_\Gamma(K) = \frac{1}{\Gamma 2^{\Gamma - 1}} \sum_{n=0}^{n_{\max}} \binom{\Gamma}{n} (\Gamma - 2n) \tanh[(\Gamma - 2n)K], \tag{6}$$

where $n_{\max}$ takes values $\Gamma/2$ for even $\Gamma$ or $(\Gamma-1)/2$ in the case of odd $\Gamma$. Note that the coefficient of the term corresponding to products of even numbers of spins in the expansion of $\langle \tanh(\Sigma_i^\Gamma K_1^{(i)} \sigma_1^{(i)}) \rangle$ is identically zero, for any value of $\Gamma$. Thus the other term in Eq. (5), $g(p,K,t)$, comes from three-spin and higher-order-spin products. It is possible, in principle, to include higher correlations, at the expense of going to coupled equations of motion [30] for higher-spin moments, but this is not the route we have taken here. Neglecting third-order and higher-spin correlations and defining the coefficient of the single-spin expectation value in the presence of bond randomness, $a(p,K)$, via

$$a(p,K) = \sum_{\Gamma=1}^{\Gamma_0} \binom{\Gamma_0 - 1}{\Gamma - 1} p^{\Gamma} (1-p)^{\Gamma_0 - \Gamma} a_\Gamma(K), \tag{7}$$

we see that we can write the equation of motion for the magnetization at a given site as

$$\left(1 + \frac{d}{dt}\right) m_0(t) = a(p,K) \sum_{i=1}^{\Gamma_0} m_1^{(i)}. \tag{8}$$

Taking the Laplace transform of Eq. (8) we obtain

$$(1+s) m_0[s] = a(p,K) \sum_{i=1}^{\Gamma_0} m_1^{(i)}. \tag{9}$$

### B. Clustering scheme

In this subsection we will motivate and construct a type of clustering scheme, which preserves the interconnectivity of the nodes which will be eventually decimated (see Fig. 3). We will then obtain the equations of motion for the magnetizations of the corner spins on these clusters.

First we would like to make more explicit our claim that Migdal-Kadanoff bond moving drastically underestimates the number of loops in the system in high dimensions. Making a change of variables to $y = \tanh(\beta J)$, we may write the *static* RG transform for the cluster shown spanning an edge of the MK bond-moved lattice in Fig. 3(c), for $d$ dimensions, and with arbitrary rescaling factor $\lambda$ as

$$y' = \frac{N y^\lambda}{1 + (N-1) y^{2\lambda}}, \tag{10}$$

where $N = \lambda^{d-1}$. The "rule of thumb" leading to this equation is as follows [31]: in the numerator appears the $N$ parallel paths connecting two sites of the cluster which will not be decimated (corner spins). These paths contribute $y^\lambda$, where $\lambda$ is the number of links along the one-dimensional chains of spins connecting the corner spins. The second term in the denominator counts the number of loops in the cluster, with $y^{2\lambda}$ corresponding to the product of $y$'s around one complete loop. It can easily be checked numerically that for large $d$, the fixed point of this equation, $y^*$ will become very small compared to unity, in which case the second term in the denominator can be neglected. The approximate fixed-point equation then yields $y^* = 1/N^{1/(\lambda-1)}$. The RG eigenvalue then becomes $\Lambda \equiv dy'/dy|_{y^*} = \lambda$, and one trivially obtains $\nu = \ln\lambda / \ln\Lambda = 1$ for large $d$. Thus, to be able to escape this trivial result, one should modify the RG procedure in such a way that contributions from the linear parts of the graph do not completely dominate the loops.

With this in mind, let us return to the modified bond moving scheme which we proposed in the Introduction and Fig. 3(d). Note that each unit cell of the $d$-dimensional lattice contributes to $d$ such clusters, which, under coarse graining (i.e., decimation of the "middle spins" and rescaling), go to the renormalized bonds in the direction of the basis vectors. Clearly, for the $d$-dimensional hypercubic lattice without dilution, one has to further specify the clusters connecting the corner spins which remain after the decimation step. We will base our construction on the clue provided by Fig. 3(d), where we see that the pair of middle spins in the cluster for $d=2$ are connected to each other. At the risk of overestimating the number of loops at higher dimensions, we propose that after bond moving, all the $N = 2^{d-1}$ middle spins within each cluster be completely interconnected as shown in Fig. 8. We will implement the transformation for the scaling parameter $\lambda = 2$. For $d=2$ and $d=3$, the number of loops incorporated into the $d$ clusters exactly accounts for the number of loops contained in the original unit cell—namely, 4 and 36.

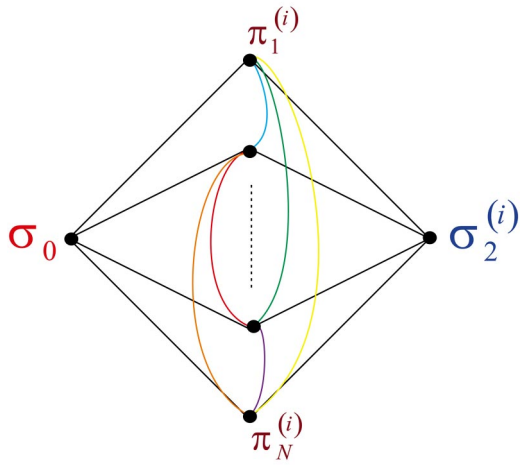


FIG. 8. (Color online) The cluster in our scheme which will, in the coarse-grained lattice for $\lambda=2$, go to the bond connecting the "corner spin" $\sigma_0$ to its nearest neighbor in the $i$th direction—namely, $\sigma_2^{(i)}$. The intermediate ("middle") spins to be decimated will be denoted by $\pi_j^{(i)}$, $j=1,\ldots,N=2^{d-1}$, from now on. We postulate that all the "middle" spins are connected to each other to estimate better the number of different paths, or loops, contributing to the spin correlations.

Thus, we will adopt the convention that in the bond-moved lattice, in the $i$th direction, $i=1,\ldots,\Gamma_0$, between the corner spins $\sigma_0$ and $\sigma_2^{(i)}$, there exists a cluster containing $N=\lambda^{d-1}$ middle spins denoted by $\pi_j^{(i)}$, with $j=1,2,\ldots,N$, as illustrated in Fig. 8.

We should mention here that one could start with the clusters depicted in Fig. 8, with $N$ middle spins, and proceed to construct a hierarchical lattice by successively replacing each bond with such a cluster, *ad infinitum* [12,13,31]. (We can always define an effective dimension via $2^{d_{\rm eff}-1}=N$.) The results of the RG transformation which we will effect here will be exact on this hierarchical lattice, and so will the exponents which we obtain for the pure and the diluted cases.

When we introduce bond randomness, the bonds appearing in the cluster in Fig. 8 will, of course, be present or absent with probabilities $p$ and $(1-p)$. The corner spins may have a maximum number $\Gamma_{0,c}=\Gamma_0 N$ of nearest neighbors at this stage. The maximum number of nearest neighbors the middle spins may have is $\Gamma_{0,m}=N+1$. The distribution of the number of nearest neighbors is thus given by

$$P(\Gamma')=\sum_{n=0}^{\Gamma'_{\rm max}}\binom{\Gamma'_{\rm max}}{n}(1-p)^n p^{\Gamma'_{\rm max}-n}\delta(\Gamma'-(\Gamma'_{\rm max}-n)), \tag{11}$$

where $\Gamma'_{\rm max}$ is $\Gamma_{0,c}$ for the corner spins and $\Gamma_{0,m}$ for the middle spins.

The equation of motion for the expectation value of the $j$th middle spin in the $i$th direction now becomes

$$\left(1+\frac{d}{dt}\right)\langle\pi_j^{(i)}\rangle=\gamma(p,K)\left[m_0+m_2^{(i)}+\sum_{k\neq j}\langle\pi_k^{(i)}\rangle\right], \tag{12}$$

where $m_2^{(i)}\equiv\langle\sigma_2^{(i)}\rangle$ and $\gamma(p,K)$ comes from the configuration average given by

$$\gamma(p,K)=\sum_{\Gamma'=1}^{\Gamma_{0,m}}\binom{\Gamma_{0,\rm m}-1}{\Gamma'-1}p^{\Gamma'}(1-p)^{\Gamma_{0,m}-\Gamma'}a_{\Gamma'}(K). \tag{13}$$

If we write down the equation of motion for the expectation value of the corner spins, we obtain

$$\left(1+\frac{d}{dt}\right)m_0(t)=A(p,K)\sum_{i=1}^{\Gamma_0}\sum_{j=1}^{N}\langle\pi_j^{(i)}\rangle, \tag{14}$$

where $A(p,K)$ comes from the configuration average:

$$A(p,K)=\sum_{\Gamma'=1}^{\Gamma_{0,c}}\binom{\Gamma_{0,\rm c}-1}{\Gamma'-1}p^{\Gamma'}(1-p)^{\Gamma_{0,c}-\Gamma'}a_{\Gamma'}(K). \tag{15}$$

### C. Obtaining the dynamical RSRG equations

Now we are ready to perform the decimation by eliminating the middle spins. The aim is to rewrite the equation of motion for the corner spins in terms of their $\lambda$th neighbors. In our case, with $\lambda=2$, this means obtaining the equation of motion for $m_0$ in terms of the $m_2^{(i)}$'s. For this purpose we will write down the equations for the expectation values of the middle spins $\langle\pi_j^{(i)}\rangle$'s in the $i$th direction and sum over $i$. The right-hand side contains only terms in $m_0$ and $m_2^{(i)}$. We find

$$\left[1+\frac{d}{dt}-(N-1)\gamma(p,K)\right]\sum_{j=1}^{N}\langle\pi_j^{(i)}\rangle=N\gamma(p,K)\left[m_0+m_2^{(i)}\right]. \tag{16}$$

Thus we obtain the equation of motion for the magnetizations of the middle spins in the $i$th direction, in terms of the corner spin magnetizations $m_0$ and $m_2^{(i)}$. If we multiply the equation of motion (14) for $m_0$ by $[1+d/dt-(N-1)\gamma(p,K)]$, we obtain

$$\left[1+\frac{d}{dt}-(N-1)\gamma(p,K)\right]\left(1+\frac{d}{dt}\right)m_0(t)=A(p,K)\sum_{i=1}^{\Gamma_0}\left[1+\frac{d}{dt}-(N-1)\gamma(p,K)\right]\sum_{j=1}^{N}\langle\pi_j^{(i)}\rangle. \tag{17}$$

Using Eq. (16) we get

$$\left[1+\frac{d}{dt}-(N-1)\gamma(p,K)\right]\left(1+\frac{d}{dt}\right)m_0(t)=A(p,K)\sum_{i=1}^{\Gamma_0}N\gamma(p,K)[m_0+m_2^{(i)}] \tag{18}$$

and

$$\left[\left(1+\frac{d}{dt}\right)^2-(N-1)\gamma(p,K)\left(1+\frac{d}{dt}\right)-N\Gamma_0 A(p,K)\gamma(p,K)\right]m_0(t)=NA(p,K)\gamma(p,K)\sum_{i=1}^{\Gamma_0}m_2^{(i)}. \tag{19}$$

Since by assumption we are near the critical line, not only are all the magnetizations small, but the time derivatives are also small due to critical slowing down. Keeping only up to linear order in the time derivatives [1] to be able finally to compare with Eq. (8), we obtain,

$$\left\{[1-(N-1)\gamma(p,K)-N\Gamma_0 A(p,K)\gamma(p,K)]+[2-(N-1)\gamma(p,K)]\frac{d}{dt}\right\}m_0(t)=NA(p,K)\gamma(p,K)\sum_{i=1}^{\Gamma_0}m_2^{(i)}. \tag{20}$$

Now let us write this equation in a familiar form

$$\left\{1+\frac{2-(N-1)\gamma(p,K)}{1-\gamma(p,K)[N-1+N\Gamma_0 A(p,K)]}\frac{d}{dt}\right\}m_0=\frac{NA(p,K)\gamma(p,K)}{1-\gamma(p,K)[N-1+N\Gamma_0 A(p,K)]}\sum_{i=1}^{\Gamma_0}m_2^{(i)}. \tag{21}$$

Taking the Laplace transform we get

$$\left\{1+\frac{2-(N-1)\gamma(p,K)}{1-\gamma(p,K)[N-1+N\Gamma_0 A(p,K)]}s\right\}m_0[s]=\frac{NA(p,K)\gamma(p,K)}{1-\gamma(p,K)[N-1+N\Gamma_0 A(p,K)]}\sum_{i=1}^{\Gamma_0}m_2^{(i)}. \tag{22}$$

We see that the equation of motion (22) is in the same form as Eq. (9). We identify the second term in the curly brackets as the renormalized Laplace variable $\tilde{s}$. The coefficient in front of the summation appearing on the right-hand side we identify as the coefficient $a(\tilde{p},\tilde{K})$, expressed in terms of the renormalized variables $\tilde{p}$, $\tilde{K}$. We thus obtain the RG equation for the time from

$$\frac{\tilde{s}}{s}=\frac{2-(N-1)\gamma(p,K)}{1-\gamma(p,K)[N-1+N\Gamma_0 A(p,K)]} \tag{23}$$

and the implicit RG transformation for $K$ from

$$a(\tilde{p},\tilde{K})=\frac{NA(p,K)\gamma(p,K)}{1-\gamma(p,K)[N-1+N\Gamma_0 A(p,K)]}\equiv R(p,K), \tag{24}$$

where $a(p,K)$ is given by Eq. (7). The transformation for the renormalized occupation probability $\tilde{p}$ is found by calculating the probability $f(p)$ of an unbroken path from the spin $\sigma_0$ to $\sigma_2^{(i)}$ through the cluster in the $i$th direction and is thus independent from $K$. Thus, the fixed-point value for the occupation probability satisfies

$$p^*=f(p^*). \tag{25}$$

Note that this implies that at each stage of the decimation, the distribution of the bond strengths is replaced by a distribution of the initial binary form, Eq. (2), with the renormalized parameters $\tilde{p}$ and $\tilde{K}$ [32]. This may hide from view certain features of the random fixed point associated with the full distribution [22,23].

The fixed point of the dynamical RG transformation for $K$ is found from

$$a(p^*,K^*)=R(p^*,K^*), \tag{26}$$

where $p^*$, found from Eq. (25), should be substituted. We can evaluate the correlation critical exponent $\nu$ from

$$\left.\frac{d\tilde{K}}{dK}\right|_{p^*,K^*}=\left.\left[\frac{\partial R(p,K)}{\partial K}\Big/\frac{\partial a(\tilde{p},\tilde{K})}{\partial\tilde{K}}\right]\right|_{p^*,K^*}=\lambda^{-\nu}, \tag{27}$$

and the dynamical critical exponent $z$ is given by

$$\left.\frac{\tilde{s}}{s}\right|_{p^*,K^*}=\lambda^z. \tag{28}$$

## III. RESULTS AND DISCUSSION

In the foregoing we have presented the generalized dynamical RSRG framework for the kinetic Ising model on diluted $d$-dimensional lattices with a random number of nearest neighbors, motivated by an interest in the scaling behavior of relaxation times on random networks.

For the case with no bond dilution, we calculated the correlation length critical exponent $\nu$ and dynamical critical exponent $z$ with our new scheme of clustering in $d$-dimensional hypercubic lattices and found that $\nu$ converges to 0.63 and $z$ converges to 1.6 for large $d$ values as shown in Figs. 4 and 5. The numerical values are given in Table I. We submit that these results are qualitatively better than those obtained by the conventional Migdal-Kadanoff bond moving scheme, Figs. 1 and 2. Here, just as for the conventional Migdal-Kadanoff bond moving scheme, these results for the critical point and the correlation exponent found from the dynamical RSRG scheme differ from those found directly from the fixed point of a static RSRG transformation. We report the results for the correlation length exponent $\nu_{\text{static}}$ in Table I.

Our scheme yields dynamical critical exponent values $z=2.13$ and $z=2.09$ in two and three dimensions, as well as the percolation exponent $\nu_p$. We report our results in Table II. We see that the agreement between the known value of $\nu_p=4/3$ in two dimensions is about as good as the result in three dimensions, with the best Monte Carlo values being reported as $\nu_p=0.88$ [33]. The values of the dynamical critical exponents are in very good agreement with recent Monte Carlo results, as summarized in Table III.

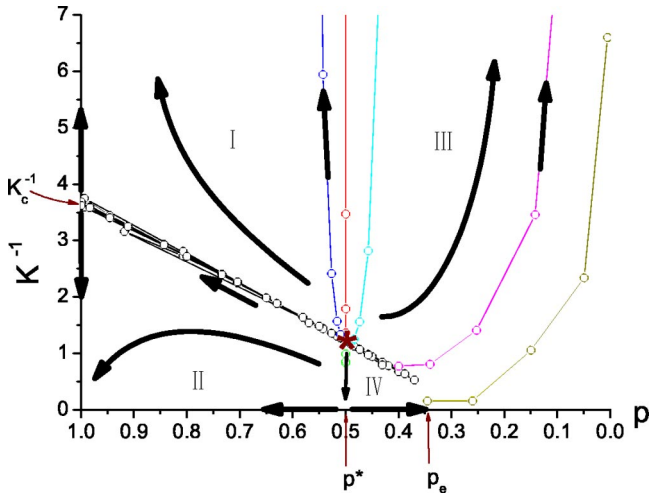


FIG. 9. (Color online) The phase diagram, $K^{-1}=k_BT/J$ versus $p$, for $d=2$. There is an unstable fixed point at $p^*=0.5$, $(K^*)^{-1}=1.22$, indicated by * in the figure. The line of points extending to the right of the unstable fixed point is explained in the text. The flow from region IV is to the high-temperature, $p=0$ fixed point. Thus the line from $(p^*,T^*)$ to the percolation fixed point, $(p^*,0)$ is a first-order phase transition line. The critical behavior on the phase boundary extending from * to the pure Ising fixed point at $T_c$ at $p=1$ is determined by the latter point.

For the bond-diluted case, we first computed the RG flows for $d=2$ and $d=3$ (see Figs. 9 and 10). Due to the high-temperature approximation made in the determination of the RG transformations, these flows are well defined on the disordered side of the separatrix and also for temperatures less than, but close to, the transition temperatures, but not in the whole ordered region. Nevertheless, their examination is crucial to obtain the phase diagrams correctly.

For $d=2$, we find that the regions I and II flow, respectively, to the disordered and ordered fixed points at $p=1$, $T\to\infty$ and $p=1$, $T=0$. The flow on the separatrix itself is to the pure Ising fixed point indicated by $T_c$ on the $p=1$ line. Note that the line of fixed points of the equation $a(\tilde{p},K^*)=R(p,K^*)$ extending to the right of $(p^*,K^*)$ and coming down to zero at $p_e$ is not a phase boundary, although it lies close to the separatrix for $p\geqslant p^*$ and passes through an unstable fixed point at $(p^*,K^*)$. For $p<p^*$, we find that in both regions III and IV, the flows are to the attractive disordered fixed point at $p=0$, $T\to\infty$. The line connecting the unstable fixed point at $p^*=0.5$, $(K^*)^{-1}=1.22$, indicated by * in the figure, to the percolation fixed point, $(p^*,0)$ is therefore a first-order phase transition line, separating a region with finite magnetization from one with zero magnetization. This suggests that the unstable fixed point $(p^*,K^*)$ is a tricritical point (TCP), with a first-order phase boundary connecting this point to the percolation fixed point $p^*=0.5$ at $T=0$. We have checked that along the separatrix, from the unstable disorder fixed point to the pure Ising fixed point, the magnetization is zero. [We have also checked that the mean-field-type equation for the equilibrium order parameter $m_0$, which one may obtain from Eq. (3) by setting all the magnetizations to be the same and interpreting the brackets as purely configuration averages, gives a second-order phase transition in this interval, with the expected value of the order parameter critical exponent $\beta=0.5$.] The values of $\nu_{\text{dynamic}}$ and $z$ at the TCP are 0.48 and 2.16, respectively. (Similar unexpected features have arisen in other phase diagrams obtained via RSRG treatments of systems with random bonds [34].)

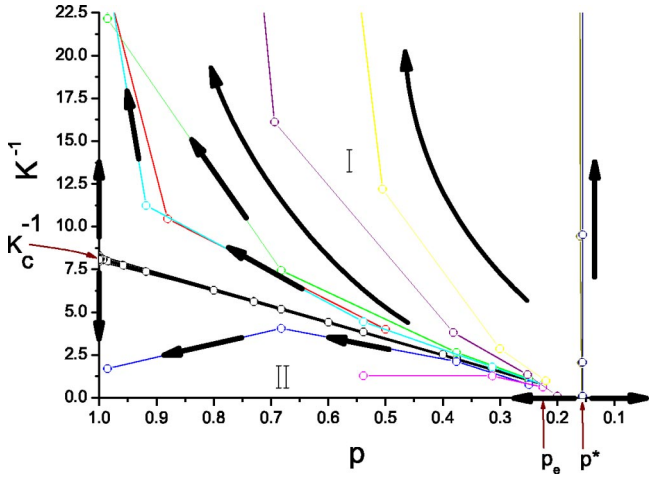


FIG. 10. (Color online) The phase diagram, $K^{-1}=k_BT/J$ versus $p$, for $d=3$. There is no fixed point other than the pure Ising one for nonzero temperatures. Thus the critical behavior of the system is determined by the pure Ising fixed point for finite $T$. Note that the phase boundary comes down to zero temperature at a concentration $p_e$ which is greater than the percolation fixed point $p^*$.

For $d=3$ the dynamical RG results for $\nu$ gives, via $\alpha=2-d\nu$, once again a positive value for $\alpha$ (although the static result is negative, as can be readily computed from the values in Table I). However, we now find that there is no $K$ which the RG relation $a(p^*,K^*)=R(p^*,K^*)$ is satisfied. Examining the flow diagram in Fig. 10, we see that the phase separation line comes down to $T=0$ at some $p_e>p^*$, precluding such a fixed point. The flow in regions I and II is respectively, to the disordered and ordered fixed points, while on the separatrix it is once more to the pure Ising fixed point. For very low temperatures, near $p_e$, the details of the phase boundary are not available, due to the same difficulty as we encountered for $d=2$.

Since Monte Carlo simulations are plagued by crossover effects along critical lines, we also computed effective critical exponents $z_{\text{eff}}$ along the critical line. For each given $p$ along this line, we solved for a $p$-dependent fixed point of $K$ under the transformation in Eq. (24) which now becomes $a(f(p),K^*)=R(p,K^*)$. We then substitute $p$ and $K^*(p)$ in Eq. (23) and evaluate $z_{\text{eff}}$ from $(\tilde{s}/s)_{p,K^*}=\lambda^{z_{\text{eff}}}$. We find that for $d=2$, $z_{\text{eff}}$ first increases from 2.13 at $p=1$ until 2.25 at $p=0.75$ and then decreases to 2.01 at $p_e$ as shown in Fig. 6. For $d=3$ the dependence on $p$ is again nonmonotonic, starting from 2.09 at $p=1$, increasing to 2.69 at $p=0.4$ and decreasing to 2.54 at $p_e$ (see Fig. 6).

The calculation of the dynamical critical exponent $z$ for the bond- (or site-) diluted quenched random Ising model is currently the subject of numerical studies. Recent Monte Carlo simulations for the dynamical critical exponent $z$ for the bond-diluted and quenched random Ising model have only yielded an effective exponent $z_{\text{eff}}$ varying between 0.59

to 0.27 along the critical line [35]. These values are markedly lower than the values found here.

For $d \geqslant 4$, considering either the static or the dynamic values of the correlation length exponent in Table I, we find a negative specific heat exponent from the hyperscaling relation $\alpha = 2 - d\nu$. This suggests, although not conclusively [26], that on all these lattices, the pure Ising fixed point will be attractive within this approach. Under dilution, the critical behavior of the second-order phase boundary will be determined by the pure Ising fixed point. In Table I, we also display the dynamical critical exponent $z$ at the pure Ising fixed point for these values of $d$.

It should be recalled that the exponents we have reported so far are *exact* on hierarchical lattices [12,13,31] generated by the cluster shown in Fig. 8. From the discussion above, we conclude that for effective dimension $d_{\text{eff}} \geqslant 4$, pure Ising behavior will be observed on the critical line for $T > 0$ and $p > p_e(d)$ on these hierarchical lattices.

We would like to end with a remark regarding the connection of the present calculation to scale-free and random networks [2], respectively. We have already mentioned that the vertices on hierarchical lattices have a nonuniform number of nearest neighbors, $k$. In fact, for the undiluted case, our hierarchical lattice is a scale-free network with a power-law degree distribution $n(k) \sim k^{-\gamma}$, where $\gamma = 1 + \ln[2 + (N-1)/2]/\ln N$ and $N$ is the number of "middle spins" in Fig. 8. We may now construct random hierarchical lattices by randomly diluting each bond, with a uniform bond occupation probability $p$. This yields, for small $p$, the asymptotic degree distribution $\propto \exp[-(1-p)k]/k!$ which is Poissonian. Thus, in the limit of small $p$ and with respect to its degree distribution, the diluted hierarchical lattice is indistinguishable from the classical random network of Erdös and Renyi [36]. We thus conclude that our results also extend to scale-free and random networks.

## ACKNOWLEDGMENT

A.E. would like to gratefully acknowledge partial support from the Turkish Academy of Sciences.

[1] M. Suzuki, K. Sogo, I. Matsuba, H. Ikeda, T. Chikama, and H. Takano, Prog. Theor. Phys. **61**, 864 (1979).
[2] S. N. Dorogovtsev and J. F. F. Mendes, Adv. Phys. **51**, 1079 (2002).
[3] A. A. Migdal, Zh. Eksp. Teor. Fiz. **69**, 1457 (1975).
[4] L. P. Kadanoff, Ann. Phys. **100**, 359 (1976).
[5] M. Droz, Phys. Lett. **73A**, 407 (1979).
[6] M. Droz and A. Malaspinas, J. Phys. C **13**, 4365 (1980).
[7] A. C. D. van Enter, R. Fernandes, and A. Sokal, J. Stat. Phys. **72**, 879 (1994).
[8] J. Bricmont, A. Kupainen, and R. Lefevre, Commun. Math. Phys. **194**, 359 (1998).
[9] It has recently been demonstrated that the critical trajectory of the so-called "hierarchical Ising model" Hamiltonian on which the block-spin transformation is exact (not to be confused with "hierarchical lattices" considered in this paper) does converge to the Gaussian fixed point under repeated renormalization group transformations in four dimensions: T. Hara, T. Hattori, and H. Watanabe, Commun. Math. Phys. **220**, 13 (2001).
[10] K. G. Wilson and J. Kogut, Phys. Rep., Phys. Lett. **12C**, 75 (1974).
[11] D. J. Amit, *Field Theory, the Renormalization Group and Critical Phenomena*, International Series in Pure and Applied Physics (McGraw-Hill, New York, 1978).
[12] A. N. Berker and S. Ostlund, J. Phys. C **12**, 4961 (1979).
[13] M. Kaufman and R. B. Griffiths, Phys. Rev. B **24**, 496 (1981).
[14] D. Stauffer, Physica A **244**, 344 (1997).
[15] M. P. Nightingale and H. W. J. Blöte, Phys. Rev. Lett. **76**, 4548 (1996).
[16] Z. B. Li, L. Schülke, and B. Zheng, Phys. Rev. Lett. **74**, 3396 (1995).
[17] K. B. Lauritsen and N. Ito, Physica A **202**, 224 (1994).
[18] C. Mülker, D. W. Heerman, J. Adler, M. Gofman, and D. Stauffer, Physica A **193**, 540 (1993).
[19] N. Ito and Y. Ozeki, in *Computer Simulation Studies in Condensed Matter Physics*, edited by D. P. Landau, S. P. Lewis, and H.-B. Schüttler (Springer, Heidelberg, 2001), Vol. XII, pp. 175,cited in N. Ito and Y. Ozeki, Physica A **321**, 262 (2003).
[20] N. Ito, Physica A **192**, 604 (1993).
[21] M. Droz and A. Malaspinas, Helv. Phys. Acta **53**, 241 (1980).
[22] D. Andelman and A. N. Berker, Phys. Rev. B **29**, 2630 (1984).
[23] S. Wiseman and E. Domany, Phys. Rev. E **58**, 2938 (1998).
[24] H. G. Ballesteros, L. A. Fernández, V. Martin-Mayor, A. Muñoz Sudupe, G. Parisi, and J. J. Ruiz-Lorenzo, Phys. Rev. B **58**, 2740 (1998) and references therein.
[25] A. B. Harris, J. Phys. C **7**, 1671 (1974).
[26] W. Janke and M. Weigel, Phys. Rev. B **69**, 144208 (2004).
[27] J.-M. Luck, Europhys. Lett. **24**, 359 (1993).
[28] A. Efrat and M. Schwartz, Phys. Rev. E **62**, 2952 (2000); A. Efrat, *ibid.* **63**, 066112 (2001).
[29] R. J. Glauber, J. Math. Phys. **4**, 294 (1963).
[30] R. Dickman, Phys. Lett. A **122** 463 (1987).
[31] B. Derrida, J.-P. Eckmann, and A. Erzan, J. Phys. A **16**, 893 (1983); A. Erzan, Phys. Lett. **93A**, 237 (1983).
[32] Y. M. Yeomans and R. B. Stinchcombe, J. Phys. C **12**, 347 (1979).
[33] D. Stauffer and A. Aharony, *Introduction to Percolation Theory* (Taylor & Francis, London, 1994), p. 52.
[34] A. Falicov and A. N. Berker, Phys. Rev. Lett. **76**, 4380 (1996).
[35] P. E. Berche, C. Chatelain, B. Berche, and W. Janke, Eur. Phys. J. B **38**, 463 (2004) and references therein.
[36] P. Erdös and A. Renyi, Publ. Math. (Debrecen) **6**, 209 (1959), cited by Dorogovtsev and Mendes [2].